Extended-reach access network with downstream radio-over-fiber (ROF) signal and upstream NRZ signal using orthogonal-WDM

C. W. Chow,[1,*] S. P. Huang,[1] L. G. Yang,[1] and C. H. Yeh[2]

[1]*Department of Photonics and Institute of Electro-Optical Engineering, National Chiao Tung University, Hsinchu 30010, Taiwan*

[2]*Information and Communications Research Laboratories, Industrial Technology Research Institute (ITRI), Hsinchu 31040, Taiwan*

**cwchow@faculty.nctu.edu.tw*

Abstract: We propose and demonstrate an extended-reach radio-over-fiber (ROF) access network. The double-sideband carrier-suppressed (DSCS) optical signal carries the downstream ROF signal. A continuous wave (CW) optical carrier is embedded into the DSCS optical signal and transmitted to the colorless optical networking unit (ONU)/remote antenna unit (RAU) for the upstream signal generation. At the ONU/RAU, the upstream data is orthogonally wavelength division multiplexed (WDM) onto this CW carrier; hence mitigating the cross-talk generated by the downstream signal. Analyses about the optimum power difference between the downstream and the CW signals; as well as the split-ratio are also preformed.

OCIS codes: (060.0060) Fiber optics and optical communications; (060.2360) Fiber optics links and subsystems; (350.4010) Microwaves.

References and links

1. C. W. Chow, F. M. Kuo, J. W. Shi, C. H. Yeh, Y. F. Wu, C. H. Wang, Y. T. Li, and C. L. Pan, "100 GHz ultra-wideband (UWB) fiber-to-the-antenna (FTTA) system for in-building and in-home networks," Opt. Express **18**(2), 473–478 (2010).
2. G.-K. Chang, J. Yu, Z. Jia, and J. Yu, "Novel optical-wireless access network architecture for simultaneously providing broadband wireless and wired services," Proc. OFC, Anaheim, USA, 2006, Paper OFM1D.
3. W.-Y. Lin, C.-H. Chang, P.-C. Peng, H.-H. Lu, and C.-H. Huang, "Direct CATV modulation and phase remodulated radio-over-fiber transport system," Opt. Express **18**(10), 10301–10307 (2010).
4. X. Pang, A. Caballero, A. Dogadaev, V. Arlunno, R. Borkowski, J. S. Pedersen, L. Deng, F. Karinou, F. Roubeau, D. Zibar, X. Yu, and I. T. Monroy, "100 Gbit/s hybrid optical fiber-wireless link in the W-band (75-110 GHz)," Opt. Express **19**(25), 24944–24949 (2011).
5. D. B. Payne and R. P. Davey, "The future of fiber access systems," BT Technol. J. **20**(4), 104–114 (2002).
6. C. W. Chow, C. H. Yeh, C. H. Wang, F. Y. Shih, C. L. Pan, and S. Chi, "WDM extended reach passive optical networks using OFDM-QAM," Opt. Express **16**(16), 12096–12101 (2008).
7. G. Goldfarb, G. Li, and M. G. Taylor, "Orthogonal wavelength-division multiplexing using coherent detection," IEEE Photon. Technol. Lett. **19**(24), 2015–2017 (2007).
8. A. D. Ellis and F. C. G. Gunning, "Spectral density enhancement using coherent WDM," IEEE Photon. Technol. Lett. **17**(2), 504–506 (2005).
9. C. W. Chow, C. H. Yeh, C. H. Wang, C. L. Wu, S. Chi, and C. Lin, "Studies of OFDM Signal for Broadband Optical Access Networks," IEEE J. Sel. Areas Comm. **28**(6), 800–807 (2010).
10. C. W. Chow, C. H. Yeh, L. Xu, and H. K. Tsang, "Rayleigh backscattering mitigation using wavelength splitting for heterogeneous optical wired and wireless access networks," IEEE Photon. Technol. Lett. **22**(17), 1294–1296 (2010).
11. M. Bakaul, A. Nirmalathas, C. Lim, D. Novak, and R. Waterhouse, "Hybrid multiplexing of multiband optical access technologies towards an integrated DWDM network," IEEE Photon. Technol. Lett. **18**(21), 2311–2313 (2006).
12. Y.-T. Hsueh, M.-F. Huang, S.-H. Fan, and G.-K. Chang, "A novel lightwave centralized bidirectional hybrid access network: seamless integration of RoF with WDM-OFDM-PON," IEEE Photon. Technol. Lett. **23**(15), 1085–1087 (2011).
13. J. Ma, J. Yu, C. Yu, X. Xin, J. Zeng, and L. Chen, "Fiber dispersion influence on transmission of the optical millimeter-waves generated using LN-MZM intensity modulation," J. Lightwave Technol. **25**(11), 3244–3256 (2007).

#165932 - $15.00 USD Received 11 Apr 2012; revised 23 May 2012; accepted 14 Jun 2012; published 10 Jul 2012

1. Introduction

Wireless access network play a very important role in our daily lives by providing flexible network connections to subscribers at anywhere and anytime. Recently, there is a trend in wireless communication towards increased capacity and towards supporting a wide range of broadband services. Hence radio-over-fiber (ROF) technologies have been proposed and demonstrated for transmitting the radio-frequency (RF) signals in optical domain [1–4]. Besides, the traditional fiber-optic wired access network is continue evolving to provide high capacity triple play services of voice, high-definition video and Internet. Besides, fiber-to-the-home (FTTH) using passive optical networks (PONs) have now been deployed in many different countries all over the world. A novel high capacity extended-reach wavelength division multiplexed (WDM) access architecture has been demonstrated to integrate the present metro and access networks into a single system, while at the same time could reduce the capex and opex [5,6].

To increase the capacity of the WDM access network without using additional fiber paths, increasing the spectral efficiency of the network is crucial. Orthogonal WDM scheme [7,8] is attractive since its operation speed is not limited by the electronic signal processing speed as in the case of orthogonal frequency division multiplexing (OFDM) [9]. In this work, we propose and demonstrate an extended-reach ROF access network. The proposed scheme does not need electrical up-conversion at the remote node (RN) or base station when compared with [10]. The proposed scheme also does not require multiple laser sources to generate separate signals for the ROF and upstream signals when compared with [11]. A centralized bidirectional hybrid access network integrating ROF and WDM-OFDM-PON has been proposed [12]; however it requires two optical interleavers, specific bandwidth and channel-spacing optical filter for the generation and separation of the signals respectively. In the proposed scheme, the double-sideband carrier-suppressed (DSCS) optical signal carries the downstream ROF signal. A continuous wave (CW) optical carrier is embedded into the DSCS optical signal and transmitted to the colorless optical networking unit (ONU)/remote antenna unit (RAU) for the upstream signal generation. At the ONU/RAU, the upstream data is orthogonally wavelength division multiplexed onto this CW carrier, providing an extended reach (> 60 km of single mode fiber (SMF)) transmission with mitigated cross-talk generated by the downstream signal. Analyses about the optimum power difference between the downstream and the CW signals; as well as the split-ratio of the network are also preformed.

2. Principle and experiment of the upstream signal generation using orthogonal WDM

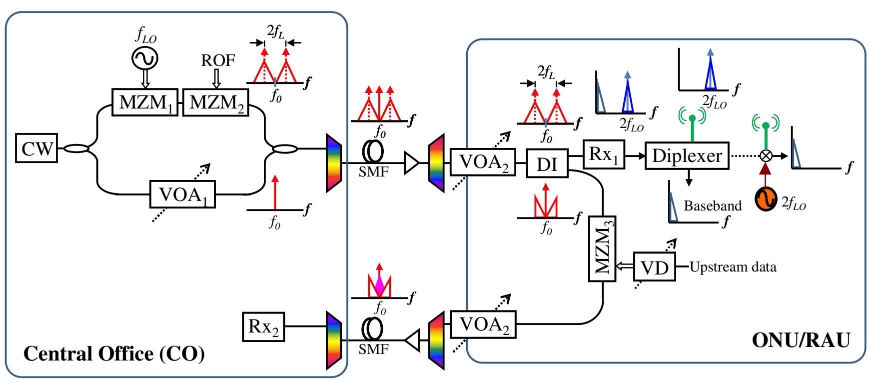

Fig. 1. Experimental setup of the extended-reach access network. Insets: optical (red figures) and RF (blue figures) spectra at different points of the network.

The experiment of the extended-reach access network is shown in Fig. 1. A CW signal (wavelength of 1550.9 nm) was first divided into two paths by a 3-dB fiber coupler. In the upper path, the first Mach-Zehnder modulator (MZM$_1$) was based at the transmission null and was electrically driven by a 5 GHz sinusoidal signal to produce two coherent optical tones

#165932 - $15.00 USD Received 11 Apr 2012; revised 23 May 2012; accepted 14 Jun 2012; published 10 Jul 2012

with frequency separation of 10 GHz. Then MZM_2 was used to encode the two optical tones with 5 Gb/s non-return-to-zero (NRZ) pseudorandom binary sequence (PRBS) 2^{31}-1 data, generating the optical DSCS ROF signal. In the lower path, the un-modulated CW signal was sent to the ONU/RAU for the generation of the upstream signal. A variable optical attenuator (VOA_1) was used to control the power of the CW signal. The schematic optical (red fig.) and RF spectra (blue fig.) are also included in the insets of Fig. 1. In later section, we will analyze the relative power difference between the distributed CW carrier and the DSCS ROF signals, and the optimum power condition was studied. Then the signals from both upper path and lower path were combined by a 3-dB coupler and then transmitted to the ONU/RAU via a pair of Gaussian-shaped arrayed waveguide grating (AWG) with insertion loss of 3 dB each; and 60 km of standard SMF (total insertion loss of 12 dB); and EDFAs with gain of 23 dBm and noise figure of 4 dB. Two VOA_2 were used before the ONU/RAU to emulate the split-ratio of the network.

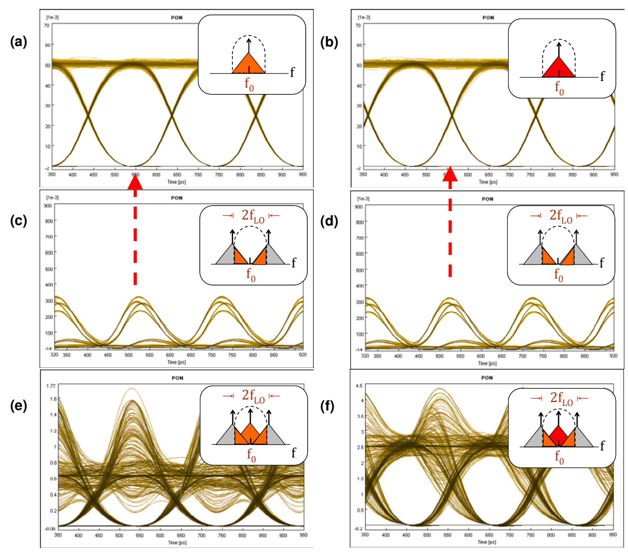

Fig. 2. Principle of orthogonal WDM for the upstream and ROF signals.

Inside the ONU/RAU, a passive optical delay interferometer (DI) of 100 ps (free spectral range (FSR) of 10 GHz) was used to optically de-multiplex the distributed CW and the ROF signals. The DI allowed the ROF signal to transmit at the upper output port, while the CW signal was transmitted at the lower output port. A receiver (Rx_1) was connected to the upper port of the DI. At the Rx_1, the coherent beating between the two optical tones generated the RF signal for wireless application, while the self-beating of the NRZ signal produced the baseband-detected signal. An electrical diplexer was used to separate these two band signals. In the experiment, the RF signal was down-converted by an RF mixer for bit-error-rate (BER) evaluation. Then the optical CW signal at the lower output port of the DI was encoded by MZM_3 to produce the upstream signal sending back to the central office (CO). At the ONU/RAU, the upstream data is orthogonally wavelength division multiplexed onto this CW carrier with mitigated cross-talk generated by the downstream ROF signal. The delay of the applied electrical signal was adjusted by an electrical variable delay (VD). BER measurements were performed for the RF-down-converted ROF, baseband-detected ROF and the upstream signals at back-to-back (B2B) and after 60 km SMF transmission respectively, showing error-free operations can be achieved in all cases. Simulations were performed using VPI Transmission Maker V7.5.

Figure 2 shows the principle of using orthogonal WDM to encode the upstream data onto the distributed CW carrier with mitigated cross-talk generated by the downstream ROF signal. In typical WDM, the wavelength channel separation should be large enough to avoid cross-

#165932 - $15.00 USD Received 11 Apr 2012; revised 23 May 2012; accepted 14 Jun 2012; published 10 Jul 2012

talk generated by adjacent channels. Figures 2(a) and (b) show the upstream NRZ signal generated using the distributed CW carrier without the cross-talk produced by the adjusted ROF channels. Figures 2(c) and (d) show the residual cross-talk from the high frequency components of the two adjacent channels (produced by the ROF signal). As these components are inside the pass-band of the optical DI and will produce cross-talk to the upstream NRZ signal. The residual cross-talks are return-to-zero (RZ) liked due to the transient components of the signal. If the condition of the orthogonal WDM is not maintained, poor upstream signal is resulted as shown in Fig. 2(e). By maintaining the orthogonal WDM with proper adjusting the delay of the applied NRZ data, the cross-talk generated by the downstream ROF signal can be mitigated. A clear open upstream eye-diagram can be achieved as shown in Fig. 2(f). Insets of Fig. 2 illustrate the corresponding schematic optical spectra.

3. Results and discussion

It is important to note that the relative power between the distributed CW signal and the DSCS ROF signal will affect the transmission performance. In this section, we first numerically studied the optimum operation condition after the 60 km SMF transmission. Figure 3 shows the simulated (using VPI Transmission Maker) Q-values (dB) of different signals against the power difference, △P (△P = power of distributed CW carrier – power of ROF). The simulation was based on the experimental setup in Fig. 1. Using higher CW power (increasing the △P) will increase the performance of the upstream NRZ signal, however, it will degrade the ROF signal, and there is a trade-off between them as shown in Fig. 3. We observe that the optimum performance of the upstream and the ROF signal was at △P ~3 dB, and this condition was used in the experiment.

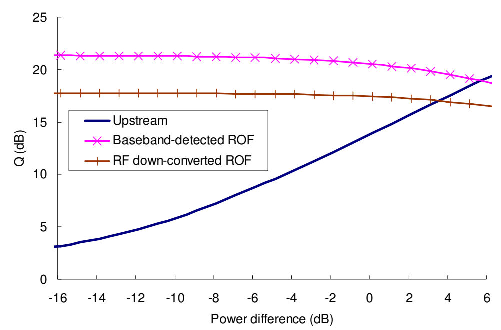

Fig. 3. Stimulated Q-values of power differences between the distributed CW and the ROF signals.

Then BER measurements were performed for the experimental setup in Fig. 1. Figures 4(a) and (b) show the BER measurements of the baseband-detected ROF signal and the RF down-converted ROF signal respectively. Power penalties of 1 dB and 2 dB were observed respectively after the extended-reach 60 km SMF transmission without dispersion compensation. The power penalties are due to the chromatic dispersion induced code-time shifting, since the same data are carried in both sidebands of the ROF signal [13]. An error-free operation can be achieved, showing that the distributed CW carrier and the ROF signal can be successfully de-multiplexed by the DI. The corresponding simulated (upper graph) and experimental (lower graph) eye-diagrams are also included in the insets, showing clear and widely open eyes in all cases. There is a good match between the simulated and experimental eye-diagrams.

The BER performance of the upstream NRZ signal is shown in Fig. 5(a). Error-free operation and wide clear open eye-diagram can be observed. This shows that the upstream NRZ signal can be successfully orthogonal wavelength division multiplexed onto the CW carrier. The transients from the ROF signal are only appeared at the crossing point of the upstream signal. Figure 5(b) shows the experimental optical spectral of the downstream ROF

#165932 - $15.00 USD Received 11 Apr 2012; revised 23 May 2012; accepted 14 Jun 2012; published 10 Jul 2012

signal and the un-modulated distributed CW carrier, while Fig. 5(c) shows the experimental optical spectra of the downstream ROF signal and the modulated upstream NRZ signal. We can see that the center wavelength suppression of the DSCS ROF signal is more than 20 dB. We can also observe that after the upstream NRZ modulation at the ONU/RAU, the CW signal is broadened due to the carrying of the upstream NRZ signal. As shown in Fig. 5(c), even thought there is a high spectral overlap between the modulated upstream and the ROF signals, error-free transmission using orthogonal WDM can be achieved.

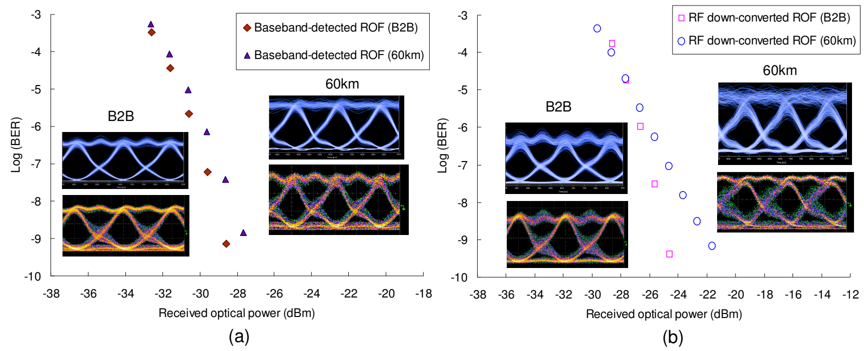

Fig. 4. BER measurements of the (a) baseband-detected and (b) RF down-converted ROF signals. Insets: corresponding simulated and experimental eye-diagrams.

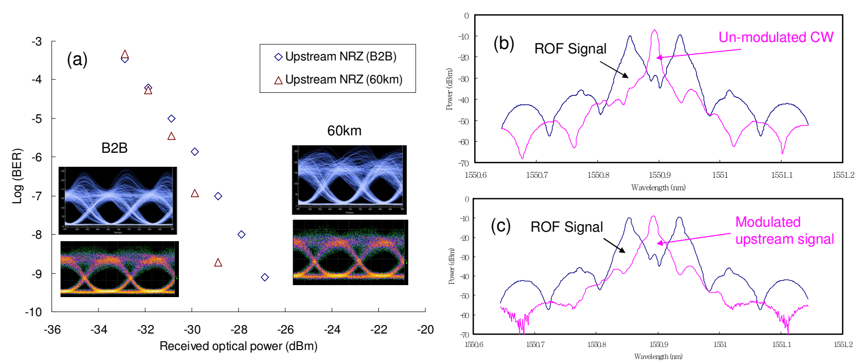

Fig. 5. (a) BER measurements of the upstream NRZ signal and (b) optical spectra of the ROF with the un-modulated CW signals and (b) optical spectra of the ROF with the upstream NRZ signals.

Then we studied the maximum split-ratio. The two VOA_2 were used to emulate the split-ratio. They were adjusted accordingly in the analysis. Figure 6 shows the measured power penalties of the three signals at different split-ratios. As the upstream NRZ signal is signal-to-noise ratio (SNR) limited, changing the split-ratio will significantly affected its performance. When the split-ratio is 128 (corresponding to the VOA attenuation of > -21 dB), the power penalty of the upstream signal will increase to 3 dB when compared with the case without the split-ratio. Much higher power penalty will be observed when the split-ratio is increase to 256 (corresponding to the VOA attenuation of > -24 dB). There is negligible power penalty in the ROF signals during these split-ratios.

#165932 - $15.00 USD Received 11 Apr 2012; revised 23 May 2012; accepted 14 Jun 2012; published 10 Jul 2012

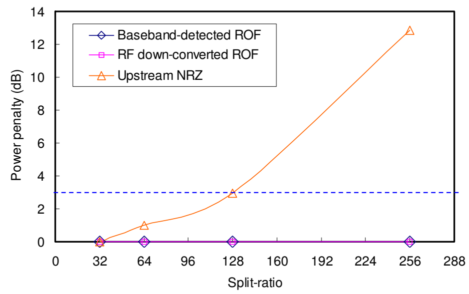

Fig. 6. Power penalties of the ROF and upstream NRZ signals at different split-ratios of the network.

We then discussed the scalability and flexibility of the proposed scheme. 60 GHz ROF signal was numerically analysis using VPI Transmission Maker. The downstream ROF DSCS signal was fixed at 60 GHz carrying 30 Gb/s data, while the upstream NRZ signals were at 30 Gb/s, 15 Gb/s and 7.5 Gb/s respectively. It is important to note that the bit-rate of the upstream NRZ signal should not be greater than half of the frequency separation of the two sidebands of the ROF DSCS signal. The DI used to de-multiplex the CW and the ROF signal was 16.6667 ps in these 3 upstream bit-rates. Figure 7(a)-(c) show the simulated eye-diagrams of the upstream NRZ signals at bit-rates of 30 Gb/s, 15 Gb/s and 7.5 Gb/s respectively. The corresponding simulated optical spectra are shown in Fig. 7(d)-(f). From the simulation results, we observed that even the bit-rate of the upstream signal decreases, the Q-values of the upstream signals are nearly the same, which is ~18 dB. This is because the residual frequency components from the ROF signal are still inside the pass-band of the DI, producing similar cross-talk to the upstream NRZ signals. By lowering the bit-rate, the time-delay requirement between the upstream NRZ and the ROF signal becomes less crucial.

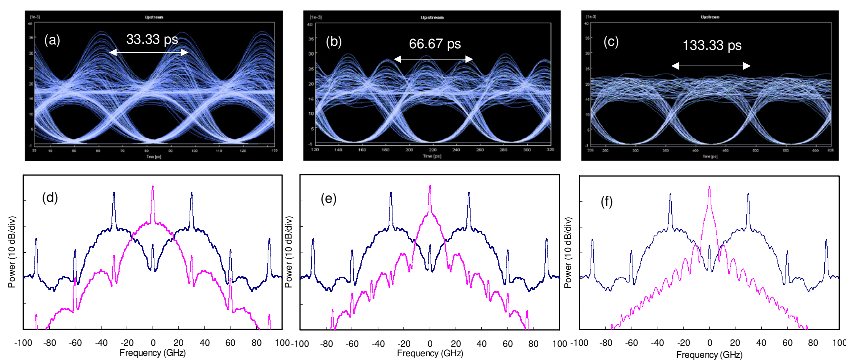

Fig. 7. Stimulated eye-diagrams of the upstream NRZ signals (a) 30 Gb/s, (b) 15 Gb/s and (c) 7.5 Gb/s; and the corresponding simulated optical spectra.

5. Conclusion

We proposed and demonstrated an extended-reach ROF access network. A DSCS optical signal carries the downstream ROF signal; together with a CW optical carrier were transmitted to the colorless ONU/RAU. At the ONU/RAU, the upstream data is orthogonally wavelength division multiplexed onto this CW carrier, providing a 60 km extended-reach transmission with mitigated cross-talk generated by the downstream signal. It can support 128 split-ratio, which is much higher than that in the present PON.

Acknowledgments

This work was financially supported by the National Science Council, Taiwan, R.O.C., under Contract NSC- 100-2221-E-009-088-MY3 and NSC-98-2221-E-009-017-MY3.

#165932 - $15.00 USD Received 11 Apr 2012; revised 23 May 2012; accepted 14 Jun 2012; published 10 Jul 2012